Formation of Mammalian Cu_8–Metallothionein *in Vitro*: Evidence for the Existence of Two $Cu(I)_4$–Thiolate Clusters†

Dean L. Pountney, Ivo Schauwecker, Jürg Zarn, and Milan Vašák*

Biochemisches Institut der Universität Zürich, Winterthurerstrasse 190, 8057 Zürich, Switzerland

Received January 26, 1994; Revised Manuscript Received May 18, 1994®

ABSTRACT: Copper accumulates in metallothionein (Cu-MT) in copper overload diseases, such as Wilson's disease and Bedlington Terriers disease. The *in vitro* formation of the Cu_{12}-MT form comprising two $Cu(I)_6(CysS)_{9,11}$ cores is well documented. However, lysosomal Cu-MT isolated from canine liver contains 8 Cu(I) ions in two proposed adamantane-like Cu_4-thiolate clusters [Freedman, J. H., Powers, L., & Peisach, J. (1986) *Biochemistry 25*, 2342]. The present studies have been carried out in an effort to learn more about the Cu(I)–thiolate cluster species formed upon the sequential incorporation of Cu(I) ions into metal-free MT from rabbit liver. On the basis of changes in the electronic absorption, circular dichroism (CD), magnetic circular dichroism (MCD), and luminescence spectra, besides the formation of a molecular species with 12 Cu(I) equivalents, evidence for the existence of a distinct MT complex with 8 Cu(I) equivalents (Cu_8-MT) was obtained. Analysis of the metal-dependent absorption envelope of Cu(I)-MT between 240 and 360 nm permitted the discrimination between predominantly CysS–Cu(I) charge-transfer (LMCT) (240–260 nm) and cluster-localized Cu(I) (d–s) transitions (260–360 nm). Accordingly, the decrease in the ratio of intensities of LMCT to d–s bands from 2.6 to 2.4 on going from 8 to 12 Cu(I) equivalents was attributed to the formation of Cu-MT species with different cysteine ligand to metal stoichiometries. The results suggest that while in Cu_{12}-MT all 20 thiolate ligands participate in metal binding, in the Cu_8-MT species between 12 and 14 cysteines take part in Cu(I) coordination. The low-temperature luminescence spectrum (77 K) of Cu_8-MT is characterized by low- and high-energy emission bands at 610 nm ($\tau \sim 130$ μs) and 425 nm ($\tau \sim 50$ μs), respectively. In contrast, the corresponding spectrum of the two Cu_6 clusters in Cu_{12}-MT exhibits only the low-energy band at 610 nm ($\tau \sim 130$ μs). The measured lifetimes (τ) are consistent with emissions from triplet excited states assigned to mixed d–s/LMCT in origin. Similar luminescence behavior has been observed with crystallographically defined inorganic $Cu(I)_6$ and $Cu(I)_4$ cluster models where it has been attributed to a shorter Cu···Cu separation in the latter case [Ford, P. C., & Vogler, A. (1993) *Acc. Chem. Res. 26*, 220]. Accordingly, the occurrence of the high-energy band in Cu_8-MT provides evidence for the existence of $Cu(I)_4$ clusters in this species. On the basis of these data, it is concluded that the Cu_8-MT species contains two $Cu(I)_4(CysS)_{6-7}$ clusters and is thus analogous to that isolated from canine liver (Bedlington Terriers disease). It is suggested that the formation of distinct Cu_8- and Cu_{12}-MT species reflects the relative concentrations of copper and protein present in solution.

Metallothioneins (MT)[1] are a class of low molecular mass (6–7 kDa), cysteine-rich proteins which bind with high affinity d^{10} metal ions such as Zn(II), Cd(II), and Cu(I). Although they occur ubiquitously in eukaryotic cells, the biological function of these proteins remains unclear. One suggested role for MT lies in the handling of heavy metal ions in the maintenance of cellular homeostasis of essential trace metals, such as Zn(II) and Cu(I), and in the detoxification of physiologically harmful metals, such as Hg(II) and Cd(II) (Kägi & Schäffer, 1988; Hamer, 1986; Pountney et al., 1994). The involvement of MT in the regulation of physiological copper levels is of particular importance in some clinical disorders, such as Wilson's disease and Bedlington Terriers disease, the pathologies of which are linked to copper overload (Scheinberg & Sternlieb, 1984; Bremner, 1993).

In the case of Wilson's disease, inherited defects in the synthesis of a copper-binding protein result in abnormally high concentrations of copper, especially in the liver and kidney (Bull et al., 1993; Woods & Colon, 1989). It has been shown that copper accumulates in these organs largely as the Cu-MT complex (Hunziker & Sternlieb, 1991; Mulder et al., 1992). Indeed, the induction of increased MT biosynthesis through the administration of zinc salt is used as an alternative treatment for mild copper overload in instances when conventional chelation therapy is inappropriate (Scheinberg & Sternlieb, 1984; Brewer & Zuzbasiyan-Gurkan, 1989).

Structural studies of mammalian Cu(I)-MT have focused on the mode of copper binding, the geometry of the metal binding sites, and their organization. The stoichiometry of copper binding to mammalian MTs has been the subject of a number of independent investigations, yielding a variety of different results. Thus, the protein isolated from the hepatic cytosol of acutely copper-overloaded individuals appears to contain about 12 Cu atoms (Hunziker & Sternlieb, 1991). This value is consistent with previous titration studies of either the metal-free or Cd/Zn-containing protein with Cu(I), where spectroscopic features developing upon copper addition were observed to saturate at around 12 copper equivalents (Nielson et al., 1985; Gasyna et al., 1988; Stillman 1992; Li & Weser, 1992). The metal binding sites of the $Cu(I)_{12}$-MT form prepared *in vitro* have been probed by a variety of spectroscopic,

† This work was supported by Swiss National Science Foundation Grants 31-25655.88 and 31-32572.91.

* Author to whom correspondence should be addressed.

® Abstract published in *Advance ACS Abstracts*, July 15, 1994.

[1] Abbreviations: CD, circular dichroism; MCD, magnetic circular dichroism; MT, metallothionein; apo-MT, metal-free metallothionein; LMCT, ligand-to-metal charge transfer; CC, cluster centered; DTNB, 5,5′-dithiobis(2-nitrobenzoic acid).

0006-2960/94/0433-9699$04.50/0

chemical, and physical techniques including EXAFS (Nielson & Winge, 1984; Stillman, 1992; Nielson et al., 1985; Winge, 1987; George et al., 1986, Abrahams et al., 1986; Li et al., 1990; Li & Weser, 1992). It has been concluded that the 12 Cu(I) ions are partitioned into two similar Cu_6 clusters, i.e., $Cu(I)_6(CysS)_{9-11}$, located in the N-terminal and C-terminal domains of the protein, respectively, with metal ions being both trigonally and digonally coordinated by cysteine thiolate ligands (Nielson & Winge, 1985; Pickering et al., 1993). Furthermore, *in vitro* binding of a total of 14–15 Cu(I) equivalents to mammalian MTs has also been reported (Zelazowski et al., 1989). This $Cu(I)_{14}$-MT species is thought to involve weaker, secondary binding of about two Cu(I) ions to non-cysteine ligands (Li & Weser, 1992). In contrast to the $Cu(I)_{12}$- and $Cu(I)_{14}$-MT forms, mammalian MT containing approximately 8 Cu(I) ions has been isolated from hepatic lysosomes of an animal model for mild cellular copper overload (Bedlington Terriers disease) (Johnson et al., 1981). In this protein, copper–sulfur and copper–copper distances calculated from EXAFS data (Freedman et al., 1986) have suggested the presence of adamantane-like $Cu(I)_4(CysS)_x$ clusters analogous to the M_3CysS_9 and M_4CysS_{11} clusters established for MTs containing divalent metal ions, e.g., Zn(II), Cd(II), and Co(II) (Messerle et al., 1992; Otvos & Armitage, 1980; Schultze et al., 1988; Robbins et al., 1991; Bertini et al., 1989). To date, the Cu_8-MT form has only been reported *in vivo*.

On the basis of these reports, it would appear that two stable Cu-MT complexes containing 8 and 12 Cu(I) ions are formed *in vivo*. In the present study, we have sought to examine whether MT binds Cu(I) in each of these two different complexes in response to different environmental copper concentrations. An extensive investigation of the spectroscopic properties of Cu(I)-MT complexes formed in the presence of differing concentrations of the Cu(I) ion has been conducted. On the basis of changes in the electronic absorption, circular dichroism (CD), magnetic circular dichroism (MCD) and luminescence spectra, besides the formation of molecular species with 12 and 14 Cu(I) equivalents, evidence for the existence of a distinct MT complex with 8 Cu(I) equivalents was obtained. Analysis of the corresponding spectral properties of the $Cu(I)_8$-MT form suggests structural features similar to those reported for the Cu_8-MT form isolated in the *in vivo* studies.

MATERIALS AND METHODS

MT-1 was isolated as the Cd,Zn-containing protein from rabbit liver after induction by subcutaneous injection of cadmium sulfate, as described (Vašák, 1991a; Comeau et al., 1993). The metal-free protein was prepared by acidification of the native material followed by gel permeation chromatography (Sephadex G-50) at pH 2 (Vašák, 1991b). Cu(I)-MT complexes were prepared by offering known equivalents of Cu(I) ions as the stable ($[Cu^I(CH_3CN)_4]ClO_4$ complex (Hemmerich & Sigwart, 1963) in 5 mM HCl/20% acetonitrile with stirring to the apoprotein in 10 mM HCl/5% acetonitrile, after which the pH was raised to 7.4 with 0.5 M Tris base. The absence of any Cu(II) in the freshly prepared Cu(I) stock solutions (20 mM) was confirmed by EPR measurement (Varian E-6; at 77 K). All solutions were degassed prior to use by freeze–pump–thaw cycling, and all manipulations were carried out in a nitrogen-purged glovebox. Samples were transferred directly to a stoppered quartz cuvette for spectroscopic measurements. Protein concentrations were typically 1–3 μM for the room temperature luminescence experiments and about 100 μM for other measurements. The concentration of apoprotein was determined spectrophotometrically (ϵ_{220} = 47 300 M^{-1} cm^{-1}), and copper concentrations were determined using atomic absorption spectroscopy (Instrumentation Laboratory, IL Video 12). The free cysteine contents of the apoprotein (20 ± 1) and of the $Cu(I)_8$-MT species (7 ± 1) were determined by reaction of an aliquot with DTNB, as described (Jocelyn, 1987).

Electronic absorption spectra were recorded using a Cary (Model 3) spectrophotometer. CD and MCD measurements were made using a Jasco (Model J-500C) spectropolarimeter interfaced with an IBM PS-2 microcomputer and equipped with a 1.5-T electromagnet for room temperature MCD measurements. Corrected luminescence spectra at 292 and 77 K and decay data were obtained using a SPEX fluorolog spectrofluorimeter fitted with the 1934C phosphorimeter accessory using a 45° detection geometry. Quantum efficiencies for room temperature emission spectra were determined using quinine sulfate as a secondary standard. For low-temperature luminescence measurements, samples were contained in 2-mm i.d. stoppered quartz tubes and immersed in a cylindrical quartz Dewar vessel filled with liquid nitrogen. Phosphorescence spectra were recorded at 77 K on the microcrystalline frozen samples using a 100-μs delay and a 300-μs acquisition window.

The Gaussian analysis of the difference absorption spectrum of the $Cu(I)_8$-MT complex was made using the computer program Peakfit (Jandel, Inc.) run on an IBM PS-2 microcomputer.

RESULTS

UV–Visible Absorption. The UV–visible absorption spectra of Cu(I)-MT complexes are characterized by the appearance of metal-dependent features in the UV region (Beltramini & Lerch, 1983; Lerch, 1983; Gasyna et al., 1988; Stillman, 1992; Li & Weser, 1992). The broad absorption envelope starting at about 400 nm and extending into the far-UV shows prominent shoulders at around 262 and 295 nm, the latter becoming less well resolved with more than 8 Cu(I) equivalents (Figure 1A). The intensity of the band at approximately 262 nm increases more or less linearly with increasing Cu(I) equivalents up to around 8 Cu(I) equivalents, reaching a maximum with a metal to protein stoichiometry of 12 (Figure 1A, inset). In contrast, the low-energy feature at about 295 nm increases in direct proportion to the Cu(I)/apo-MT ratio throughout the titration. A detailed analysis of the origins of these spectral features is given below [see Analysis of the $Cu(I)_8$-MT Species]. It should be noted that the lack of aromatic amino acids in MT results in a featureless absorption spectrum of the metal-free protein with no absorption intensity above 250 nm (Figure 1 A, bottom curve). Furthermore, no absorption of the Cu(I)–acetonitrile complex was observed in the spectral region presented when added to the sample buffer in the absence of protein.

Circular Dichroism. Intense dichroic bands develop in the CD spectrum of Cu(I)-MT, the positions of which parallel the features observed in the absorption spectrum (Figure 1A,B). The form of the CD spectrum is essentially unchanged with up to 8 Cu(I) equivalents and is characterized by positive and negative maxima at (+) 260 nm, (–) 283 nm, (+) 308 nm, (–) 325 nm, and (+) 357 nm and apparent isodichroic points at 342 and 273 nm. On going from 8 to 12 Cu(I) equivalents, slight shifts to higher energy occur in the positions of all extrema (Figure 1B). The CD spectrum of the $Cu(I)_{12}$-MT species is similar to that reported previously (Rupp & Weser, 1978; Stillman, 1992; Li & Weser, 1992). The

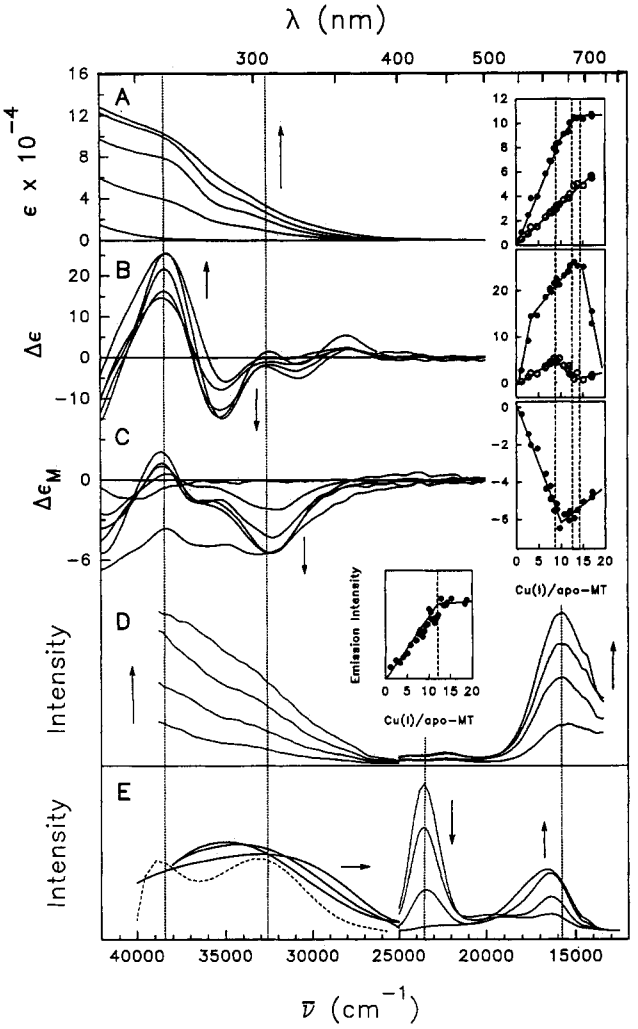

FIGURE 1: Cu(I) titration of metal-free rabbit liver MT-1. Representative examples of (A) absorption, (B) CD, (C) MCD, and corrected luminescence spectra at 292 K (D) and 77 K (E). Arrows indicate increasing Cu(I) equivalents: (A) 0, 4, 8, 12, 14; (B) and (C) 0, 4, 8, 10, 12, 14; (D) 4, 8, 10, 12; (E) 8, 4, 11, 14 (emission) and 8, 11, 14 (excitation) Cu(I) equivalents. Luminescence emission spectra are with excitation at 318 nm, and excitation spectra are detected at 600 nm (solid lines) or at 425 nm [dashed line, 8 Cu(I) equivalents]. Phosphorescence spectra (E) are normalized by the total area under the emission envelope. Inset panels illustrate the effect of Cu(I)/apo-MT ratio [0–20 Cu(I) equivalents] on (A) the absorption at 262 nm (solid circles) and at 295 nm (hollow circles), (B) the CD at 262 nm (solid circles) and at 357 nm (hollow circles), (C) the MCD at 309 nm, and (D) the room temperature luminescence at 600 nm. For further details see text.

variation in dichroic intensity of the well-resolved positive features at around 260 and 357 nm with respect to the Cu(I)/apo-MT ratio is illustrated in Figure 1B (inset). Thus, a clear maximum is observed in the magnitude of the band at around (+) 260 nm after the addition of 12 Cu(I) equivalents, with an inflection occurring at around 4 Cu(I) equivalents. The intensity of this feature drops sharply when more than 14 Cu(I) equivalents are added. The magnitude of the band at about (+) 357 nm attains a maximum with approximately 8–9 Cu(I) equivalents, disappearing altogether when more than 14 Cu(I) equivalents are added.

Magnetic Circular Dichroism. The MCD spectrum of Cu(I)-MT is dominated by two intense negative dichroic features at around 241 and 309 nm (Figure 1C), the latter band corresponding to a positive maximum in the CD spectrum. Other less intense bands are observed at about (+) 260 nm and (–) 274 nm. Similarly to the CD spectra, the positions of these extrema are virtually unaffected with increasing Cu(I)/apo-MT stoichiometries up to about 8 Cu(I) equivalents, with approximate isodichroic points at around 245 and 271 nm. Only minor differences in the relative intensities of these features are observed on going from 8 to 12 Cu(I) equivalents (Figure 1C), followed by a dramatic blue shift (ca. 50 nm) of the lower energy band at 309 nm with more than 12 equivalents (data not shown). The variations in magnitudes of the MCD bands with increasing Cu(I) equivalents added are analogous to those observed in the CD spectrum, with the feature at 260 nm saturating at 12 Cu(I) equivalents and that at about 309 nm reaching a maximum at around 8–9 equivalents (Figure 1C, inset). The negative band at around 241 nm is present in all MCD spectra and appears to increase in intensity roughly linearly up to around 20 Cu(I) equivalents (Schauwecker, 1993).

Table 1: Luminescence Properties of Cu(I)-MT and Cu(I)$_4$ and Cu(I)$_6$ Polyhedra[a]

	high-energy band[b]		low-energy band[b]			
	λ_{max} (nm)	τ (μs)	λ_{max} (nm)	τ (μs)	λ_{max} (nm)[c]	Φ_{eff} (rt)[d]
Cu_8-MT	425	49	610	128	295	0.0091
Cu_{12}-MT	–[e]		600	129	305	0.0108
$Cu_4I_4py_4$[f]	438	23	619	26	330	0.09
Cu_6mtc_6[f]	–[e]		767	14	347–475	

[a] All data are at 77 K except where noted. For details see Materials and Methods. [b] Emission spectra with Cu(I)-MT excitation at 318 nm. [c] Excitation spectra. [d] Room temperature. [e] Not observed. [f] py = pyridine; mtc = di-*n*-propylmonothiocarbamate; Ford and Vogler (1993).

Room Temperature Luminescence. Representative examples of the luminescence emission and excitation spectra of Cu(I)-MT complexes are shown in Figure 1D. The emission spectra are characterized by a broad metal-dependent band with a maximum at approximately 630 nm and a small shoulder at 695 nm. A very weak emission band was also detected at 430 nm, the intensity of which follows a similar dependence with respect to the Cu(I)/apo-MT ratio as the much more intense feature observed at a similar wavelength in the low-temperature luminescence spectra (see below). No differences in the positions of these bands were detected at room temperature throughout the titration. A maximum in emission intensity was observed with excitation at 318 nm, with a slight shift in the emission maximum toward lower energy (ca. 5 nm) occurring when excitation was at wavelengths below 285 nm (Schauwecker, 1993). The excitation spectra obtained by monitoring the emission intensity at 630 nm are similar in form to the corresponding absorption spectra, with poorly resolved shoulders at around 320 and 270 nm discernible with less than 8 Cu(I) equivalents. The large Stokes shift observed is typical for the emission of Cu(I) complexes. The intensity of the room temperature emission of Cu(I)-MT reaches a maximum with 12 Cu(I) equivalents, consistent with previous studies by Li and Weser (1992) (Figure 1D, inset). Quantum efficiencies determined for Cu(I)-MT (0.01 ± 0.001, see Table 1) do not vary significantly with the Cu(I)/apo-MT ratio and are in the same range as those reported previously for Cu(I)-MTs from yeast and fungi (Byrd et al., 1988; Beltramini et al., 1987).

Luminescence at 77 K. The low-temperature luminescence spectra of Cu(I)-MT complexes are characterized by low- and high-energy emission bands at 600–610 and 425 nm with $\tau \sim 130$ and 50 μs, respectively (see Figure 1E and Table 1), consistent with their originating from triplet excited states. In all cases, the luminescence decayed according to a single exponential function. Since the phosphorescence spectra were obtained on microcrystalline, frozen solutions using front-face detection, no direct quantification of the emission intensity

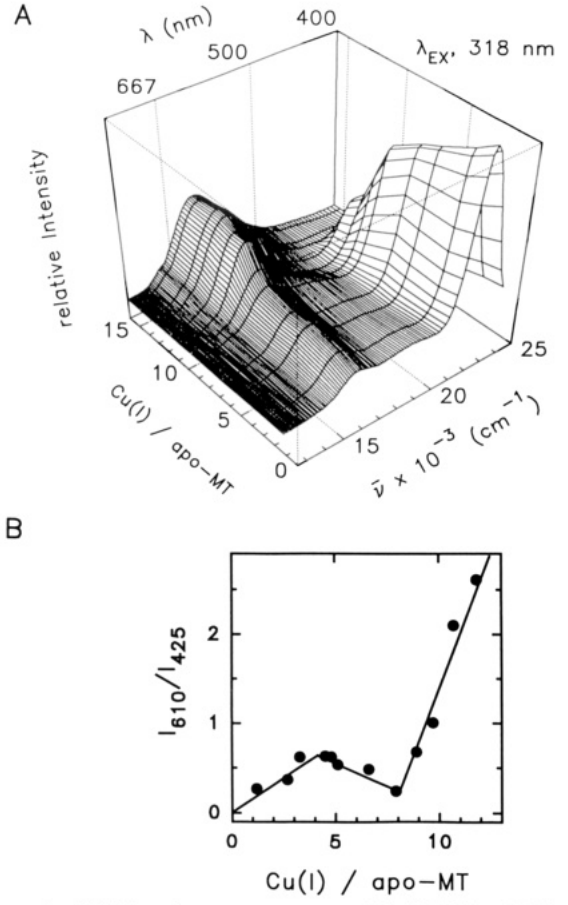

FIGURE 2: (A) Phosphorescence spectra of Cu(I)-MT at 77 K as a function of increasing Cu(I)/apo-MT ratio. Spectra are normalized by the total area under the emission envelope. (B) Ratio of relative emission intensity at 610/425 nm *vs* Cu(I)/apo-MT stoichiometry. Conditions are as in Figure 1E.

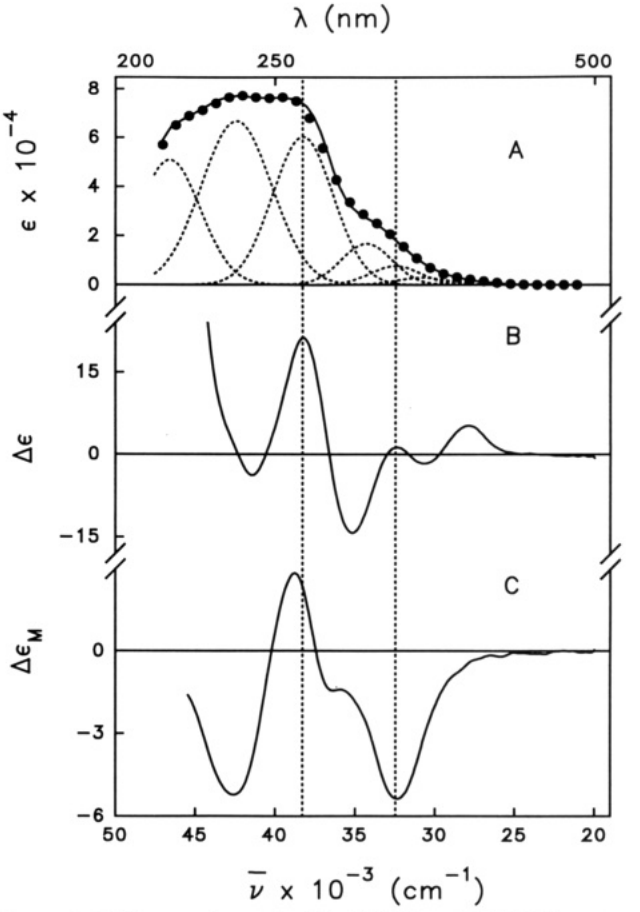

FIGURE 3: Difference absorption (A), CD (B), and MCD (C) spectra of $Cu(I)_8$-MT *vs* apo-MT (solid lines). Dashed lines in (A) illustrate individual Gaussian-resolved bands with the overall fit shown as solid circles. Conditions for spectra are as in Figure 1A–C.

in terms of the concentrations of the Cu-MT complexes is possible. However, as the respective luminescence lifetimes (τ) of both low- and high-energy emission features are essentially invariant throughout the titration, luminescence spectra normalized by area can be used to represent better the changes in their relative intensities with increasing Cu(I) added (Figure 2A). The relative intensity of the high-energy band at 425 nm diminishes rapidly after 8 Cu(I) equivalents and is absent in the spectra above 12 Cu(I) equivalents in which only the 610-nm band is present. This trend is more clearly illustrated when the ratio of intensities of these two features is plotted *vs* Cu(I)/apo-MT stoichiometry (Figure 2B), where clear turning points are observed with 4 and 8 Cu(I) equivalents. The excitation spectra obtained by monitoring the emission intensity at 610 nm show a broad envelope with a maximum centered at about 300 nm, which undergoes a slight red shift with increasing Cu(I)/apo-MT stoichiometry (Figure 1E). In contrast, when the 425-nm band is monitored, the excitation spectrum displays poorly resolved bands at 260 and 305 nm, the latter occurring in the position of the strong (–) 309 nm MCD band (Figure 1). Thus, the excitation spectra are similar whether the high- or the low-energy emission maximum is the monitoring wavelength, although better resolution of the individual components within the envelope is observed when detecting at 425 nm.

Similar trends were observed in the titration data obtained at pH 2 (prior to pH increase) as those descibed above at pH 7.4 (data not shown). In order to rule out local trapping of the Cu(I) ions added, several titration points were repeated starting with apo-MT dissolved in 0.5 M HCl, conditions under which no binding of Cu(I) to MT occurs (Weser & Rupp, 1979). No differences in the corresponding spectra at pH 7.4 were observed compared to those obtained when starting from pH 2.

Analysis of the $Cu(I)_8$-MT Species. The absorption, CD, and MCD difference spectra for $Cu(I)_8$-MT *vs* apo-MT are presented in Figure 3. The difference absorption envelope is deconvoluted into a series of overlapping Gaussian-shaped bands, based in part on the positions of resolved bands observed in the difference CD and MCD spectra. The spectrum can be divided into two distinct low- and high-energy regions, respectively. Thus, a number of low-intensity absorption bands are present in the region from 26 000 to 36 000 cm^{-1} which show relatively strong CD and MCD features, whereas three intense high-energy transitions are resolved between 36 000 and 46 000 cm^{-1} which exhibit comparatively weaker CD and MCD. These two defined parts of the electronic spectrum are dealt with separately.

High-Energy Region. In the high-energy region of the difference absorption envelope Gaussian-shaped bands are resolved at 262, 236, and 215 nm. The first two bands exhibit corresponding features in the difference CD and MCD spectra, confirming the presence of more than two electronic transitions. The transition at 262 nm has an extinction coefficient $\epsilon_{262} = 7 \times 10^3\ M^{-1}\ cm^{-1}$ per Cu(I) and a dissymmetry factor $g\ (\Delta\epsilon/\epsilon) = 3.5 \times 10^{-4}$, indicating an electric dipole allowed transition (Mason, 1983). In a series of Cu(I) halide model complexes, similar optical features have been observed, with the energy of the longest wavelength transition following the order of the electronegativity of the ligand, i.e., $Cl^- > Br^- > I^-$. This behavior has been ascribed to greater admixing of the metal d orbitals with the halide p orbitals in the bromide and iodide

salts, resulting in the predominantly LMCT character of these transitions (Allred, 1969; Jørgensen, 1970). By analogy with divalent d^{10} metal complexes, the energy of the first (lowest energy) charge-transfer transition should reflect the difference between the semiempirically derived optical electronegativities of ligand and metal ion. According to Jørgensen's proposal, the position of the first allowed absorption band ($\bar{\nu}$, expressed in cm^{-1}) is given by the simple expression:

$$\bar{\nu} = 30000[\chi_{opt}(L) - \chi_{opt}(M)] \quad (1)$$

where $\chi_{opt}(L)$ and $\chi_{opt}(M)$ are the optical electronegativities of the ligand (L) and the metal (M), respectively. On the basis of a correlation between $\chi_{opt}(L)$ and the position of the first (lowest energy) LMCT bands in metal derivatives of proteins containing cysteine ligands, a value of 2.6 for the optical electronegativity of cysteine thiolate, $\chi_{opt}(RS^-)$, has been derived (McMillin, 1978; Vašák et al., 1981; Henehan et al., 1993). Substituting the energy of the first resolved band of Cu$_8$-MT, $\bar{\nu}$ = 38 200 cm^{-1}, together with the value for $\chi_{opt}(RS^-)$ in eq 1, a value of 1.33 for $\chi_{opt}(Cu(I))$ is obtained. This calculated value for Cu(I), lying between $\chi_{opt}(Hg(II))$ = 1.50 and $\chi_{opt}(Cd(II))$ = 1.27 (Jørgensen, 1970), correlates well with the order of the degree of covalency of the metal–thiolate bond, i.e., Zn(II) < Cd(II) < Cu(I) < Hg(II), consistent with the predominantly CysS–Cu(I) LMCT assignment.

An independent support for this assignment is provided by X-ray photoelectron measurements on sulfur in MTs containing a variety of different metal ions, i.e., Zn(II), Cd(II), Hg(II), and Cu(I) (Sokolowski et al., 1974). In our previous studies on Zn$_7$-, Cd$_7$-, and Hg$_7$-MT, a linear dependence has been established between the measured CysS $2p_{1/2,3/2}$ core electron binding energy, reflecting the degree of covalency of the CysS–metal bond, and the position of the first (lowest energy) CysS–Me(II) LMCT transition (Vašák et al., 1981). This linear relationship should also hold in the case of the Cu-MT complex. Indeed, on the basis of the measured binding energy of the CysS $2p_{1/2,3/2}$ electrons (161.9 eV) the predicted energy of the first electric dipole allowed transition of Cu(I)-MT at 38 700 cm^{-1} corresponds well with the experimental value of 38 200 cm^{-1} (262 nm), thus confirming the LMCT origin of this transition.

Low-Energy Region. The CD spectra in the low-energy region of Cu$_8$-MT show unusually strong CD bands at (–) 325 and (+) 357 nm, which are present as a tailing in the absorption spectrum [ϵ_{357} = 120 M^{-1} cm^{-1} per Cu(I)]. The 357-nm transition has a dissymmetry factor g ($\Delta\epsilon/\epsilon$) of 3.5 × 10^{-3}, an order of magnitude higher than that of the charge-transfer bands described above, indicating that this transition is magnetic dipole allowed, electric dipole forbidden in nature. The intense MCD feature observed in this region further supports this assignment (Figure 1). In mononuclear d^{10} Cu(I) halide complexes, besides strong electric dipole allowed charge-transfer bands, no other absorption bands at longer wavelengths are observed; e.g., in the $Cu(I)Cl_3^{2-}$ complex the lowest energy band occurs at 274 nm (Stevenson et al., 1988). It is well documented, however, that in polynuclear Cu(I) complexes which exhibit relatively short Cu···Cu distances (ca. 2.8 Å) an intramolecular d^{10}–d^{10} interaction of adjacent Cu(I) ions leads to a number of excited states with largely metal character. These weak low-energy bands have been assigned to formally spin-forbidden 3d → 4s metal cluster-centered transitions (Mehrotra & Hoffman, 1978; Kyle et al., 1991; Sabin et al., 1992; Ford & Vogler, 1993). Thus, the occurrence of similar transitions in Cu(I)-MTs indicates the presence of Cu(I) polyhedra in these complexes. The assignment of this low-energy transition as essentially singlet–triplet in nature is consistent with the phosphorescence of these complexes. Furthermore, the strong coupling observed between the emissive excited states and the low-energy region of the absorption envelope, as indicated by the position of the maxima in the corresponding excitation spectra, is in agreement with a direct singlet–triplet excitation pathway.

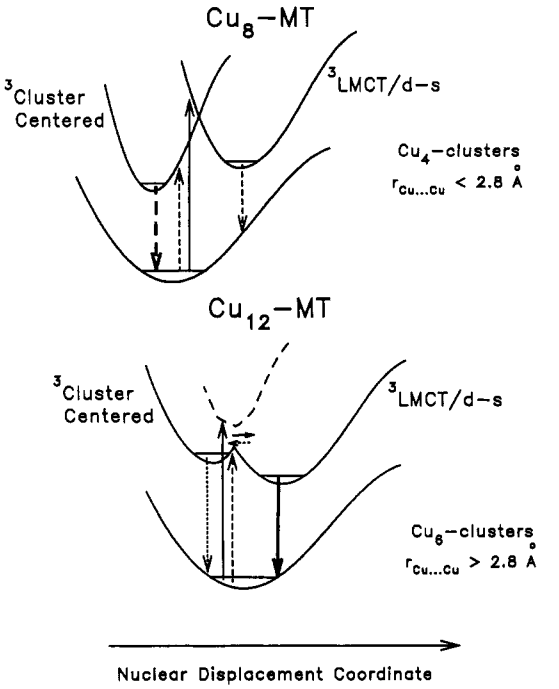

FIGURE 4: Proposed qualitative scheme describing the luminescence properties of Cu(I)$_8$- and Cu(I)$_{12}$-MT [adapted in part from Ford and Vogler (1993)].

DISCUSSION

The current work deals extensively with the spectroscopic properties of Cu-MT complexes formed in the presence of differing concentrations of the Cu(I) ion. In our titration experiments, turning points have been observed with 8, 12, and 14 Cu(I) equivalents consistent with the formation of distinct molecular species. As both Cu$_{12}$- and Cu$_{14}$-MT forms have been observed and discussed extensively in previous metal substitution studies (Winge, 1987; Stillman, 1992; Li & Weser, 1992), the discussion here will focus on the Cu$_8$-MT species.

Luminescence Properties of Cu(I)$_4$ and Cu(I)$_6$ Polyhedra. The luminescence properties of inorganic tetra- and hexanuclear Cu(I) clusters have been the subject of extensive studies (Ford & Vogler, 1993). These emissions arise from triplet excited states which are mixed d–s/LMCT in origin. Characteristically, these complexes exhibit large Stokes shifts and long emissive lifetimes (see Table 1). Moreover, while Cu$_6$ clusters exhibit only the low-energy luminiscence band at about 700 nm, high- and low-energy bands at about 430 and 620 nm, respectively, are observed in the luminiscence spectra of Cu$_4$ clusters. Detailed MO calculations for these systems predict the existence of two distinct triplet excited state manifolds, one of which, referred to as "cluster-centered" (CC), is delocalized over the metal core with almost equivalent contributions from both d–s and charge-transfer components, while the other is predominantly composed of ligand p orbitals (Avdeef & Fackler, 1978; Ford & Vogler, 1993). On the basis of both these studies and our results a qualitative scheme has been developed to describe the luminescence properties of Cu(I)$_8$- and Cu(I)$_{12}$-MT (Figure 4). In this scheme, the ^{3}CC and ^{3}LMCT/d–s excited states of each Cu-MT species are illustrated as overlapping Morse curves, with intersystem

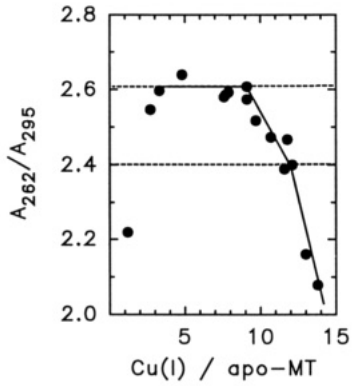

FIGURE 5: Absorbance ratio of CysS–Cu(I) LMCT (262 nm) to Cu(I)–cluster-centered (295-nm) transitions *vs* Cu(I)/apo-MT stoichiometry. See text for details.

crossing from the ^{3}CC to the ^{3}LMCT/d–s manifolds being highly favored in the case of $Cu(I)_{12}$-MT.

In the case of Cu_4 clusters, which typically show shorter Cu···Cu separations (< 2.8 Å), a high-energy barrier between the two manifolds leads to the observation of high- and low-energy emission bands, originating from both CC and ligand dominated excited states, respectively (see Table 1). The lack of a high-energy emission in Cu_6 clusters has been attributed to the longer Cu···Cu distances (>2.8 Å) generally encountered in such complexes, resulting in a lower energy barrier between the two excited states. Thus, the presence of a high-energy emission band is characteristic of the shorter Cu···Cu separations (< 2.8 Å) observed in tetranuclear Cu(I) complexes (Ford & Vogler, 1993). By analogy with these model studies, we conclude that the observation of both high- and low-energy emission bands at 425 and 610 nm, respectively, in the luminescence spectra of the $Cu(I)_8$-MT complex at 292 and 77 K is due to the existence of two Cu_4 clusters. Furthermore, the observation of spectral changes also at 4 Cu(I) equivalents in the absorption and luminescence titrations would be consistent with the cooperative formation of each cluster in a sequential manner. It is worth noting that the principal Cu···Cu distances determined for canine lysosomal $Cu(I)_8$-MT (2.74 Å), attributed to the existence of adamantane-like Cu_4 clusters (Freedman et al., 1986), would be in accord with our luminescence data. The absence of the high-energy feature in the luminescence spectrum of Cu_{12}-MT is in agreement with the previous EXAFS investigation which suggested the presence of two Cu_6 clusters in this form ($r_{Cu\cdots Cu} \sim 2.9$ Å) (George et al., 1986; Dance, 1986; Pickering et al., 1993).

CysS–Cu(I) LMCT and Cluster-Centered Transitions. A detailed analysis of the electronic spectrum, based on difference absorption, CD, and MCD spectroscopy combined with luminescence data, reveals the presence of two separate types of electronic transition which are CysS–Cu(I) LMCT and copper cluster-centered (CC) in origin. These transitions give rise to high- and low-energy features in the electronic absorption spectrum of Cu(I)-MT, respectively, the relative intensities of which change depending on the ratio of copper to protein (Figure 5). The magnitude of the LMCT absorption reflects the number of CysS–Cu(I) coordinating ligands, while that of the CC transitions parallels the number of bound metal ions. Accordingly, we attribute the decrease in the ratio of intensities of LMCT to CC bands from 2.6 to 2.4 on going from 8 to 12 Cu(I) to the formation of Cu-MT species with different cysteine ligand to metal stoichiometries (Figure 5). The intensity of this LMCT band reaches a maximum with 12 Cu(I) equivalents (ϵ = 110 000 M^{-1} cm^{-1}) (Figure 1A). As in the Cu_{12}-MT species all 20 cysteine residues are involved in Cu(I) binding (Stillman 1992; Li & Weser, 1992); this results in an extinction coefficient per cysteine thiolate of ca. 5 500 M^{-1} cm^{-1}. Thus, the intensity of the 262-nm LMCT transition of the Cu_8-MT form (ϵ = 73 000 M^{-1} cm^{-1}) suggests the involvement of only around 12–14 cysteine ligands. This conclusion implies the presence of approximately 6–8 free cysteine residues which are not involved in metal coordination. Supporting evidence for the existence of free sulfhydryl groups in this species is provided by their availability for modification by DTNB.

At this point the work of Nielson and Winge (1984), who demonstrated the preferential binding of about 6 Cu(I) ions to the 9 cysteine ligands of the β-domain (residues 1–31) of MT, should be discussed. In their proteolysis studies, partially Cu(I) occupied MT has been digested with subtilisin and the β-domain containing between 5 and 6 Cu(I) subsequently isolated. The stoichiometry of metal binding was determined independently both by Cu(I) saturation of the isolated β-domain and by a proteolytic protection assay in which both the α- and the β-domains were examined. In the former case, a value of between 5 and 6 Cu(I)/β-domain was found. In the proteolytic protection assay both the α- and the β-domains revealed a plateau near 5 Cu(I) equivalents with about 95% protection already with 4 Cu(I) equivalents. Although these studies clearly demonstrated a higher affinity of the β-domain toward Cu(I) ions, it would appear that the proteolysis procedure can affect the equilibria among the different Cu(I)-MT complexes. It may be noted that in the crystal structure of $Me(II)_7$-MT interdomain salt bridges exist (Robbins et al., 1991), suggesting that the two domains of the protein may not be completely independent of each other.

On the basis of the structural information obtained on the *in vitro* Cu_8-MT species and knowledge of inorganic $Cu(I)_4$–thiolate clusters, where similar Cu/thiolate stoichiometry exists

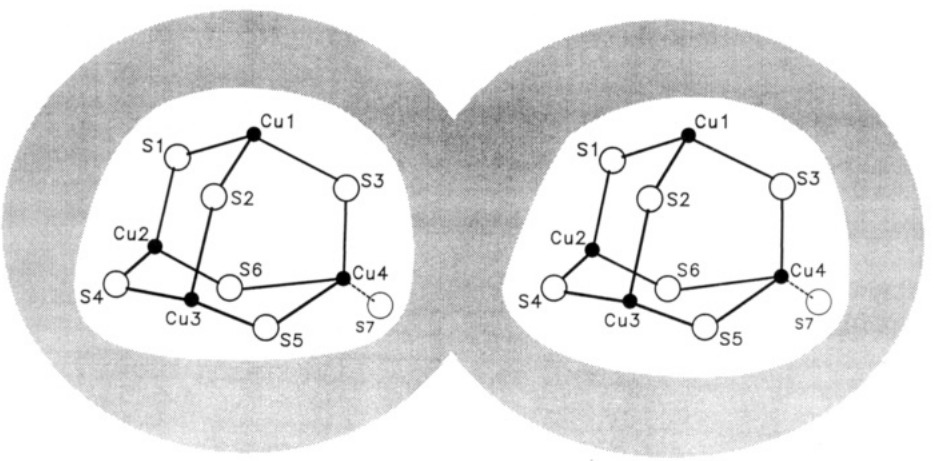

FIGURE 6: Hypothetical spectroscopic model for $Cu(I)_4(CysS)_{6-7}$ clusters in $Cu(I)_8$-MT.

(Griffith et al., 1976), a spectroscopic model of the metal cluster organization in Cu_8-MT can be developed (see Figure 6). In this proposed model the 8 Cu(I) ions are disposed in two similar, adamantane-like $Cu(I)_4(CysS)_{6-7}$ clusters. This cluster model closely resembles that suggested for lysosomal Cu_8-MT isolated from canine liver (Freedman et al., 1986). It should be noted that in the spatial structure of mammalian MT containing seven divalent metal ions, such as Zn(II), Cd(II), and Co(II), the coordinated metal ions are also organized into two metal-thiolate clusters. In this case, the N-terminal and C-terminal domains of the protein enfold the $Me(II)_3(CysS)_9$ and $Me(II)_4(CysS)_{11}$ clusters, respectively (Otvos & Armitage, 1980; Messerle et al., 1992; Schultze et al., 1988; Robbins et al., 1991; Bertini et.al., 1989). Thus, the arrangement of Cu(I) ions in Cu_8-MT, with two adamantane-like $Cu(I)_4(CysS)_{6-7}$ clusters, appears to be remarkably similar to that of the $Me(II)_7$-MT species, suggesting a predisposition of the protein to adopt a certain polypeptide fold and metal organization.

In conclusion, the formation of distinct Cu_8- and Cu_{12}-MT species containing $Cu(I)_4$– and $Cu(I)_6$–thiolate clusters, respectively, depending upon the relative concentrations of the two components present in solution has been demonstrated. Such effects, well-known in the synthesis of inorganic multimetal complexes, are uncommon in biological systems. Furthermore, the Cu_{12}-MT species obtained *in vitro* corresponds to the copper loading of MT reported as accumulating in the hepatic cytosol of Wilson's disease victims, whereas the Cu_8-MT form reported here is analogous to that isolated from lysosomes (Bedlington Terriers disease). Although the biological significance of the structural diversity of Cu-MT forms is unclear, it is tempting to speculate that the transfer of copper from the cytosolic to the lysosomal pool which occurs upon the induction of MT biosynthesis during zinc treatment of Wilson's disease (Goldfischer & Sternlieb, 1968) may result from the formation of the Cu_8-MT form concomitant with the rise in the cellular MT concentration.

ACKNOWLEDGMENT

The authors gratefully acknowledge Prof.J. H. R. Kägi for helpful discussions and Dr. F. A. Liberatore, E. I. du Pont de Nemours Inc. for the gift of the biological material.

REFERENCES

Abrahams, I. L., Bremner, I., Diakun, G. P., Garner, C. D., Hasnain, S. S., Ross, I., & Vašák, M. (1986) *Biochem. J. 236*, 585.

Allred, A. L. (1961) *J. Inorg. Nucl. Chem. 17*, 215.

Avdeef, A., & Fackler, J. P., Jr. (1978) *Inorg. Chem. 17*, 2182.

Beltramini, M., & Lerch, K. (1983) *Biochemistry 22*, 2043.

Beltramini, M., Münger, K., German, U. A., & Lerch, K. (1987) in *Metallothionein II* (Kägi, J. H. R., & Kojima, Y., Eds.) p 237, Birkhäuser Verlag, Basel.

Bertini, I., Luchinat, C., Messori, L., & Vašák, M. (1989) *J. Am. Chem. Soc. 111*, 7296.

Bremner, I. (1993) in *Metallothionein III* (Suzuki, K. T., Imura, N., & Kimura, M., Eds.) p 111, Birkhäuser Verlag, Basel.

Brewer, G. J., & Zuzbasiyan-Gurkan, V. (1989) *Dig.-Dis. 7*, 178.

Bull, P. C., Thomas, G. R., Rommens, J. M., Forbes, J. R., & Cox, D. W. (1993) *Nature Genetics 5*, 327.

Byrd, J., Berger, R. M., McMillin, D. R., Wright, C. F., Hamer, D. H., & Winge, D. R. (1988) *J. Biol. Chem. 263*, 6688.

Comeau, R. D., MacDonald, K. W., Tolman, G. L., Vašák, M., & Liberatore, F. A. (1992) *Prep. Biochem. 22*, 151.

Dance, I. G. (1986) *Polyhedron 5*, 1037 and references therein.

Ford, C. K., & Vogler, A. (1993) *Acc. Chem. Res. 26*, 220.

Freedman, J. H., Powers, L., & Peisach, J. (1986) *Biochemistry 25*, 2342.

Gasyna, Z., Zelazowski, A. J., Green, A. R., Ough, E., & Stillman, M. J. (1988) *Inorg. Chim. Acta 153*, 115.

George, G. N., Winge, D. R., Stout, C. D., & Cramer, S. P. (1986) *Inorg. Biochem. 27*, 213.

Goldfischer, S., & Sternlieb, I. (1968) *Am. J. Pathol. 53*, 883.

Griffith, E. H., Hunt, G. W., & Amma E. L. (1976) *J. Chem. Soc., Chem. Commun.*, 432.

Hamer, D. H. (1986) *Annu. Rev. Biochem. 55*, 913.

Hemmerich, P., & Sigwart, C. (1963) *Experientia 19*, 489.

Henehan, C. J., Pountney, D. L., Zerbe, O., & Vašák, M. (1993) *Protein Sci. 2*, 1756.

Hunziker, P. E., & Sternlieb, I. (1991) *Eur J. Clin. Invest. 21*, 466.

Jocelyn, P. C. (1987) *Methods Enzymol. 143*, 47.

Johnson, G. F., Morrell, A. G., Stockert, R. J., & Sternlieb, I. (1981) *Hepatology 1*, 243.

Jørgensen, C. K. (1970) *Prog. Inorg. Chem. 12*, 101.

Kägi, J. H. R., & Schäffer, A. (1988) *Biochemistry 27*, 8509.

Kyle, K. R., Ryu, C. K., & Ford, P. C. (1991) *J. Am. Chem. Soc. 113*, 2954.

Lerch, K. (1983) *Met. Ions Biol. Syst. 13*, 299.

Li, Y.-J., & Weser, U. (1992) *Inorg. Chem. 31*, 5526.

Li, Y.-J., Zhang, L., Bayer, E., Oelkrug, D., & Weser, U. (1990) *Z. Naturforsch. 45c*, 1193.

Mason, S. F. (1983) *Optical Activity and the Chiral Determinations*, Cambridge University Press, New York.

McMillin, D. R. (1978) *Bioinorg. Chem. 8*, 179.

Mehrotra, P. M., & Hoffmann, R. (1978) *Inorg. Chem. 17*, 2187.

Messerle, B. A., Schäffer, A., Vašák, M., Kägi, J. H. R., & Wüthrich, K. (1992) *J. Mol. Biol. 255*, 433.

Mulder, T. P., Janssens, A. R., Verspaget, H. W., Van Hattum, J., & Lamers, C. B. (1992) *J. Hepatol. 16*, 346.

Nielson, K., B., & Winge, D. R. (1984) *J. Biol. Chem. 259*, 4941.

Nielson, K. B., Atkin, C. L., & Winge, D. R. (1985) *J. Biol. Chem. 260*, 5342.

Otvos, J. D., & Armitage, I. M. (1980) *Proc. Natl. Acad. Sci. U.S.A. 77*, 7094.

Pickering, I. J., George, G. N., Dameron, C. T., Kurz, B., Winge, D. R., & Dance, I. G. (1993) *J. Am. Chem. Soc. 115*, 9498.

Pountney, D. L., Kägi, J. H. R., & Vašák, M. (1994) in *Metal Ligand Interactions in Biological Fluids* (Berthon, G., Ed.) Marcel-Dekker, New York (in press).

Robbins, A. H., McRee, D. E., Williamson, M., Collett, S. A., Xuong, N. H., Furey, W. F., Wang, B. C., & Stout, C. D. (1991) *J. Mol. Biol. 221*, 1269.

Rupp, H., & Weser, U. (1978) *Biochim. Biophys. Acta 533*, 209.

Sabin, F., Ryu, C. K., Ford, P. C., & Vogler, A. (1992) *Inorg. Chem. 31*, 1941.

Schauwecker, I. (1993) M.Sc. Thesis, University of Zürich.

Scheinberg, I. H., & Sternlieb, I. (1984) *Major Probl. Intern. Med. 23*, 25.

Schultze, P., Wörgötter, E., Braun, W., Wagner, G., Vašák, M., Kägi, J. H. R., & Wüthrich, K. (1988) *J. Mol. Biol. 201*, 637.

Sokolowski, G., Pilz, W., & Weser, U. (1974) *FEBS Lett. 48*, 222.

Stevenson, K. L., Braun, J. L., Davis, D. D., Kurtz, K. S., & Sparks, R. I. (1988) *Inorg. Chem. 42*, 3472.

Stillman, M. J. (1992) in *Metallothioneins* (Stillman, M. J., Shaw, C. F., III, & Suzuki, K. T., Eds.) p 55, VCH Publishers, New York.

Vašák M. (1991a) *Methods Enzymol. 205*, 39.

Vašák M. (1991b) *Methods Enzymol. 205*, 41.

Vašák, M., Kägi, J. H. R., & Hill, H. A. O. (1981) *Biochemistry 20*, 2852.

Weser, U., & Rupp, H. (1979) in *Metallothionein* (Kägi, J. H. R., & Nordberg, M., Eds.) p 221, Birkhäuser, Basel.

Winge, D. R. (1987) in *Metallothionein II* (Kägi, J. H. R., Kojima, Y., Eds.) p 213, Birkhäuser Verlag, Basel.

Woods, S. E., & Colon, V. F. (1989) *Am. Fam. Physician 40*, 171.

Zelazowski, A. J., Gasyna, Z., & Stillman M. J. (1989) *J. Biol. Chem. 264*, 17091.